Overcoming Blockage with Artificial Potential Field Assisted Mirror Reflectors for Terahertz Communications

Manus Pengnoo*, Michael Taynnan Barros‡, Lunchakorn Wuttisittikulkij*, Widhyakorn Asdornwised*
Alan Davy‡ and Sasitharan Balasubramaniam†‡

*Department of Electrical Engineering, Faculty of Engineering, Chulalongkorn University, Bangkok, Thailand.
‡TSSG, Waterford Institute of Technology, Ireland
†Dept. of Electronic and Communication Engineering, Tampere University of Technology, Finland
Email: manus.pengnoo@gmail.com, mbarros@tssg.org, sasib@tssg.org

***Abstract*—The expectation for higher capacity wireless communication links is ever increasing due to the demand for high-data intensive applications, such as multimedia streaming, as well as increased number of devices connecting to the Internet. Researchers have now recently explored regions of the spectrum that are under utilized for communications, and this is the Terahertz band (0.1 THz to 10 THz). Unlike wireless technologies today, THz frequencies come with a plethora of challenges, one of which is the requirement of constant LoS. A number of solutions have explored the use of reflectors, or even reflect-arrays, that can help assist in redirecting beams towards the mobile devices in order to avoid blockages. In this paper, we propose the use of the Artificial Potential Field concept to increase the LoS rays in a multi-ray link by controlling antenna strips selection of a base station. Our approach aims to ensure a clear THz signal path from the base station to the reflectors, and to the mobile. We also consider micro-movement events that may result in loss of connectivity, through a concept of Personal Zones that allows multiple THz rays to beam around a user. Simulation results have shown the efficiency of the Artificial Potential Field (APF) in assisting the mirrors to redirect their beams through smaller number of utilized antenna strips, which increases the signal-to-noise ratio of links.**

I. INTRODUCTION

Wireless communication systems have evolved tremendously over the years, enabling seamless connectivity to mobile users utilizing high bandwidth applications. Besides the connectivity of people, the emergence of the Internet of Things (IoT) is also witnessing devices of all scales connecting wirelessly, providing unprecedented quantity of data that is enabling efficiency for numerous applications (e.g., Healthcare, Environmental Monitoring and Protection). While this widespread connectivity has redefined how humans interact, even with machines, it has also brought along an expectation of increased capacity for future wireless communications. This expectation is not only limited to users who are facing continued emergence of new types of data-intensive services, but also communications to be established between devices and machines. The vision of the next generation wireless communications is expected to provide ultra-high-speed data communications reaching Terabit per second (Tbps), at least within small coverage areas of up to 10 m [1]. In order to achieve these targeted rates, researchers recently have investigated new spectrum for the carrier frequency that have previously been untapped. This spectrum is pushing beyond the *mm-wave* (60 GHz)[2], or even the sub-terahertz region, into the *Terahertz* (THz) bands (0.3 - 10 THz) [3]. By tapping into this spectrum, the expectation for this high capacity wireless links is new emerging services, such as multimedia base stations that can provide download links for multimedia contents in a very short period of time, or interconnection of large number of miniature devices to the Internet, also known as the Internet of Nano Things [4].

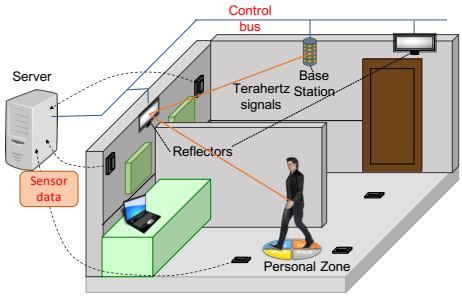

Fig. 1: Indoor architecture for wireless THz communication system with reflectors. The proposed approach requires sensors to be deployed in the room to detect obstacles and construct an Artificial Potential Field that will assist in directing the THz beams.

However, utilizing the THz band for communication leads to numerous challenges that is not traditionally found in the lower spectrum. Firstly, Line-of-sight (LoS) is a requirement between the transmitter and the receiver. A peculiar property of electromagnetic waves in the THz band is the high energy signals that scatters as they collide with rough surfaces. Thus this makes Non-Line-of-Sight (NLoS) connections very poor with a decrease of 10^6 bps in wireless links capacity [5]. The other issue is the fact that THz signals with very

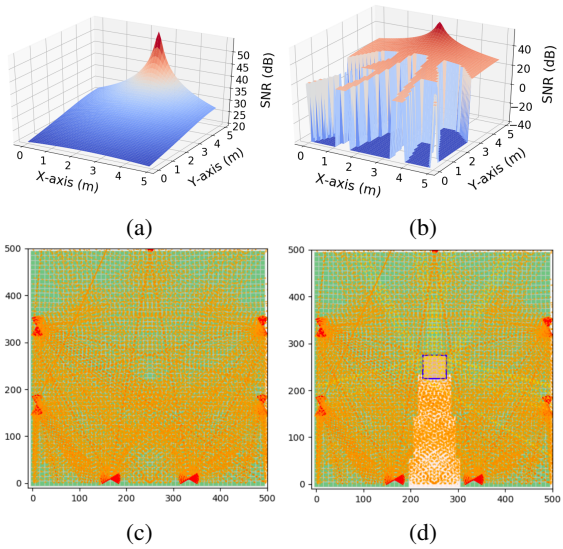

Fig. 2: Indoor THz signal strength scenarios for both cases of no-obstacle (a), and with obstacles (b). Ray tracing of signals with mirror-assistance in both scenarios of no-obstacle (c) and with obstacles (d).

short wavelengths can also suffer significant Doppler shifts. Secondly, there is significant signal attenuation due to ambient effects that is caused by free space losses. Thirdly, atmospheric effects such as molecular absorption can severely affect the signal propagation.

In this paper, we focus on the problem of NLoS propagation in the THz band, due to the presence of obstacles. Most recently, researchers have proposed the use of smart programmable reflectors or reflect-arrays to bounce LoS high frequency signals towards a mobile device [5], [6] (in essence these reflectors will act as passive transmitters). Our proposed architecture for the reflective mirror-assisted environment for THz communications is illustrated in Fig. 1. As illustrated in the diagram, the confined space includes a THz base station that consist of an array of antennas, as well as mirrors that will reflect the beam to targeted areas. Given that the THz frequency is considerably high, means that each antenna strip could be scaled to a very small size, and built from metamaterials. An example is graphene, given that its inherent properties can lower the resonant frequency by a number of folds [1]. Fig. 2 illustrates how obstacles can block the THz signals, and how the reflective mirrors can help redirect the beams, which was explored in our previous work [7]. Since THz signals will require LoS to ensure a decent level of power, the base station will require a full view of the space to know the locations of obstacles that can block or lower the quality of signals. Our proposed model considers a room equipped with sensors that can detect obstacles in order to realise an *Artificial Potential Field* (*APF*) that can increase the LoS THz rays towards an indoor location.

The objective of this paper is to determine how the APF can be used in conjunction with the THz base station in determining and selecting the best antenna strips to emit the signals towards the mobile users, in face of any obstacles. The ideal paths from the base station to the mobile device will result in an increase on the number of LoS rays and directly contribute to increase link capacity. An algorithm is also proposed that will analyze the signals towards the reflective mirrors as well as to the mobile users, and select the group of signals that can cover a `Personal Zone` around the user to ensure that any micro-movements of the mobile device will not results in loss of connectivity. Through the development of a ray-tracing simulator of the THz propagation, the paper investigates how the APF can assist in selecting a small group of antennas to emit sufficient beams to cover a personal area of a user in face of varying number of obstacles.

II. Terahertz Model

In this section we describe the multi-ray propagation model for the $0.06 - 10$ THz band developed from the following papers [5], [8], [9]. The multi-ray model considers various factors that will affect the propagation effects, including: spreading ($\Psi(f,d)$), molecular absorption ($\beta(f,d)$) and reflection ($\Gamma(f,d)$), in which f is the carrier frequency and d is the distance between the transmitter and receiver [10]. In the following, each of these effects are formulated.

1) Spreading: Spreading is represented as follows

$$\Psi(f,d) = \left(\frac{c}{4\pi f d}\right)^2, \tag{1}$$

where c is the speed of light in vacuum.

2) Molecular Absorption: The molecular absorption coefficient can be characterised as

$$k(f) = \sum_g \frac{p}{p_0}\frac{T_0}{T}\sigma^g(f), \tag{2}$$

where p is the system pressure, p_0 is the reference pressure, T_0 is the standard temperature, T is the system temperature and $\sigma^g(f)$ is the absorption cross-section. Using the *Beer-Lambert* law, we can represent the molecular absorption loss as

$$\beta(f,d) = e^{-\frac{1}{2}k(f)d}, \tag{3}$$

3) Reflection: The Kirchhoff theory is used for calculating the reflection loss of THz waves. The Fresnel reflection coefficient and the Rayleigh roughness factor are used for calculating the reflection loss, where the Fresnel reflection coefficient is:

$$R(f) = \frac{cos(\theta_i) - n_t\sqrt{1 - \left(\frac{1}{n_t}sin(\theta_i)\right)^2}}{cos(\theta_i) + n_t\sqrt{1 - \left(\frac{1}{n_t}sin(\theta_i)\right)^2}} \tag{4}$$

where θ_i is the angle of the incident wave and n_t is the refractive index of a medium. The Rayleigh roughness factor can be defined as:

$$\rho(f) = e^{-\frac{G(f)}{2}}, \tag{5}$$

and

$$G(f) = \left(\frac{4\pi\omega cos(\theta_i)}{\lambda} \right)^2, \quad (6)$$

where ω is the standard deviation of the surface roughness and λ is the free space wavelength of the incident wave. Thus, the reflection loss can be represented as

$$\Gamma(f, d') = \sum_n \Psi(f, d') \cdot \beta(f, d') \cdot R(f) \cdot \rho(f), \quad (7)$$

in which n is the number of rays, and d' is the distance between the transmitter and the mirrors plus the distance between the mirrors and the receiver.

4) Signal-Noise Ratio Model: Link budget analysis is used to model signal-noise ratio in the THz-band communication for indoor scenarios, which is in accordance to previous studies for mm-wave communication and also THz communication [2], [11]. The following formula is used for the Signal-Noise Ratio (SNR):

$$SNR = P_{tx} + G_{tx} + G_{rx} - \alpha(f, d) - \gamma - N, \quad (8)$$

where P_{tx} is the transmission power, G_{tx} is the antenna gain in the transmitter, and G_{rx} is the antenna gain in the receiver, N is the noise and γ is the loss resulting from shadowing. We use P_{tx} = 1 dBm with 7.4 dB conversion loss, G_{tx} and G_{rx} are equal to 30 dBi as in [12]. However, the receiver has a conversion gain of 8 dB with N = 7.5 dB and γ = -74 dBm. This results in

$$SNR = 127.7 - \alpha(f, d), \quad (9)$$

The path loss model can be obtained upon adding the attenuation loss of each signal propagation effect (spreading (Ψ), molecular absorption (β) and reflection (Γ)) in dB, and this is represented as:

$$\alpha(f, d) = 10 \cdot \log_{10}(\Psi(f, d)) + 10 \cdot \log_{10}(\beta(f, d)) + 10 \cdot \log_{10}(\Gamma(f, d)). \quad (10)$$

III. Artificial Potential Field-Assisted Reflectors

Since wireless communication at very short wavelength such as mm-wave or sub-millimeter wave in the THz band require LoS links, there needs to exist techniques that ensure a number of LoS rays by selecting the appropriate antenna strip from a base station for perfect transmission. In this paper, we propose the usage of sensors as guiding factors that are placed within the room to detect obstacles and their volume and surface data, as illustrated in Fig. 1. The information gathered from the sensors is necessary for our system to construct the APF. However, for this work we consider that there is a direct relationship between an obstacle sensor and the APF processing unit, but, for future works, one needs to consider machine learning processes for creating the APF from the sensor data which might be not entirely a direct process. APF has been highlighted by Vadakkepat et al. [13] for robotic real-time obstacle avoidance purpose and also a way to provide

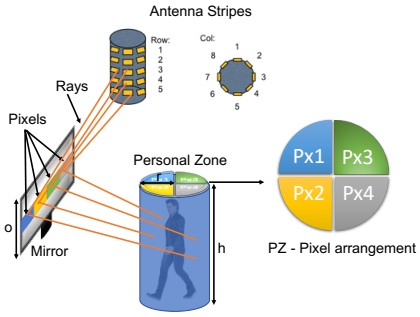

Fig. 3: The Personal Zone requires multiple THz signals to reflect from different pixels of the mirror to cover the user in order to ensure that micro-movements will not result in loss of connectivity.

communication between swarm robots in [14]. Based on this, we are inspired to use the APF as a measure for the number and location of the obstacles within the room that has the potential to block the THz signals. The aim of the APF is to determine a gradient that flows from the base station to the mirrors, and on to the location of the mobile device. This APF gradient will be used to allow the base station to select the appropriate antenna strip that will emit a beam with a sufficient SNR towards a mirror and onto the device.

A. Artificial Potential Field

APF is a reactive model that defines a spatial gradient between two points (in our case a transmitter (T_x) and a receiver (R_x)), and is obtained by differentiating a potential function $U : R^m \rightarrow R$. The potential function will have a continuous steep gradient when there are no obstacles, but in the event of any blockages, this will be indicated through the rise in the potential field (or bumps that represent the obstacles). The potential function can be constructed with the sum of attractive ($U_{att}(d)$) and repulsive ($U_{rep}(d)$) potentials, which are described in the following subsections.

B. Attractive Potential

The attractive potential ($U_{att}(d)$) is defined as a constant attractive gradient flow between the transmitter and receiver (please note that the receiver can also be the mirror), and is defined as follows

$$U_{att}(d) = \begin{cases} \frac{1}{2}\xi d^2, d \leq d^*_{goal} \\ \xi d^*_{goal} d - \frac{1}{2}(d^*_{goal})^2, d > d^*_{goal}, \end{cases} \quad (11)$$

where d is the current distance between the source and the target, and the d^*_{goal} is the target location or the receiver location, and ξ is the attraction gain that is linearly increase by a factor of one per mirror present in the room.

C. Repulsive Potential

The repulsive potential can be represented as

$$U_{rep}(d) = \begin{cases} \frac{1}{2}\eta(\frac{1}{d} - \frac{1}{Q^*})^2, d \leq Q^*, \\ 0, d > Q^* \end{cases} \quad (12)$$

where Q^* is the distance threshold for an obstacle to create a repulsion effect on the receiver, and η is the repulsion gain.

D. Total Potential Function

The total attractive potential field is the summation of all potentials from a set of M reflective objects, and is represented as follows

$$U_{att} = \sum_{i=1}^{M} U_{att_i}, \quad (13)$$

The total artificial repulsive potential field is the summation of all potentials from a set of N obstacles, and is represented as follows

$$U_{rep} = \sum_{i=1}^{N} U_{rep_i}, \quad (14)$$

Then the total potential function, which is the sum of attractive and repulsive forces can be represented as follows

$$U(d) = U_{att}(d) + U_{rep}(d). \quad (15)$$

The total potential field contains all non-negative values.

In Fig. 4, we show the integration of the APF and the THz SNR map in the room with two obstacles. Fig. 4 (a) illustrates the position of the transmitter (T_x) as well as the three obstacles, where the LoS regions are shown in green. The T_x is located at the top-center position of the room. The effect of THz SNR map with the three obstacles is shown in Fig. 4 (b). Fig. 4 (c) shows the APF based on Eq 15. Finally, Fig. 4 (d) shows how the APF is overlaid onto the THz SNR map, which shows how the gradient flows towards the mobile, and this is over the LoS region of the SNR map, avoiding the obstacles.

E. APF Signal Selection for Personal Zones

While the APF provides a means for guiding the THz signal towards the target by selecting the antenna strip, there is still another issue regarding the THz beams focus in the user's Personal Zone. The micro-movement of the users could result in a complete loss of connection with very low SNR (micro-movement is defined as change in location of the mobile device without the user changing location - such as waving an arm). Therefore, our objective is to ensure that multiple beams are projected onto the user's Personal Zone, and regardless of any micro-movement being made, the SNR can be better managed. In this subsection, we present an algorithm that selects a set of THz signal paths reflected from the mirror onto the Personal Zone for increased received SNR.

Fig. 3 depicts the concept of Personal Zones. In our model, the base station contains T_x antenna stripes, mirrors as the reflective object, and a user with a mobile device that is the R_x within the Personal Zone. Since the antenna strips can be small in size, the emitted THz beams are effectively independent signals that can focus on a specific point on the mirror (or the mobile if its LoS). Based on this, we divide the mirror into pixels, which serves as a reflective sub-area that will reflect the signal to a different point around the user's Personal Zone. We set the Personal Zone as the height of the user (h), with a radius that will represent the maximum arm's length (r). Finally, we created a THz ray scheduling algorithm that allows the selection of antenna strips that lead to a maximum of LoS rays given the available mirror resources based on the APF measurements.

Our THz ray scheduling algorithm can be visualised in Algorithm 1. Initially, the algorithm will use the APF to determine the best paths to the mirrors, as well as from the mirrors to the user. Once the paths are known, the algorithm ranks the best four THz signals that will cover the four regions of the Personal Zone (please see Fig. 3, where the four zones surrounds the user). This will ensure that the best THz signal rays will cover the Personal Zone in case of any micro-movements by the user (please note that in this paper, we do not consider any mobility of the user).

Algorithm 1 Ray scheduling algorithm for personal zone field

Define: R is the number of rays, P is the number of pixels in each mirror, T is a tuple of a ray $\in R$ and a APF U, $rank()$ is a function that selects the four rays with higher U
function SCHEDULING(M, N, R, P)
    $T_x \leftarrow$ get_D() ▷ d: euclidean distance function
    $R_x \leftarrow$ get_D()
    $d_0 \leftarrow 0$
    $U_{att} \leftarrow 0$
    $U_{rep} \leftarrow 0$
    U $\leftarrow 0$
    for $i \leftarrow 1$ to R **do**
        $P_x \leftarrow$ get_$pixel(P, M)$
        $d_0 \leftarrow D(T_x, P_x) + D(P_x, R_x)$
        for $j \leftarrow 1$ to M **do**
            $U_{att} \mathrel{+}= U_{att} + U_{att}(d_0)$
        end for
        for $k \leftarrow 1$ to N **do**
            $U_{rep} \mathrel{+}= U_{rep} + U_{rep}(d_0)$
        end for
        $T_i \leftarrow i, U$
    end for
    return $rank(T)$
end function

IV. Simulations

A THz ray tracing simulator using Python has been developed to simulate the signals and analyze the propagation and reflection of THz signal paths. In our scenario, the room is 5

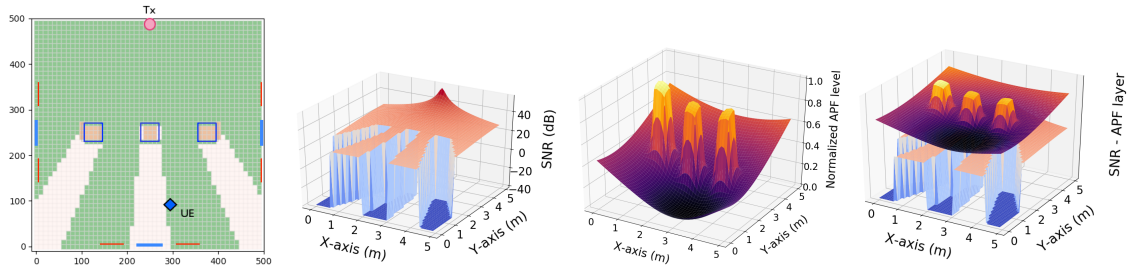

(a) (b) (c) (d)

Fig. 4: The effects of APF in an indoor scenario and its relationship with SNR. (a) The three obstacle indoor scenario and LoS regions in green and the T_x located at the top-center position. (b) SNR map. (c) APF of the three obstacle scenario. (d) Stacked surfaces of the SNR and APF maps.

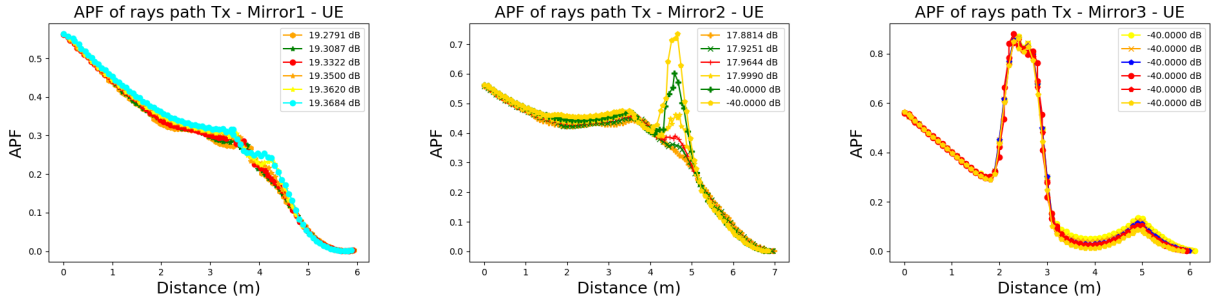

(a) (b) (c)

Fig. 5: Example of APF along the path base station-mirror-mobile device with SNR values of each individual beam for the case of 3 mirrors. (a) Mirror 1 shows that all APF gradient paths are smooth since no obstacle are in the path. (b) Mirror 2 shows two gradient paths fluctuating due to partial blockage by an obstacle, (c) Mirror 3 shows that all gradient paths are disrupted with an obstacle.

x 5 meters, and this contains three obstacles with the size of 40 x 40 cm each (Fig. 4 (d)). Mirror width is set at 50 cm. All mirrors are smooth and reflection loss is zero. The base station contains 40 antenna strips, where each is the size of 1 cm. Even though the recommended operational THz frequency based on IEEE 802.15 standard is within the 252-325 GHz spectrum [15], we aim to investigate the higher spectrum, around 1THz, for beyond 5G or 6G applications, where data rate requirements will be around 1Tpbs. We consider two mirror configurations, which is three and six mirrors (Fig. 4 (a) shows 6 mirrors in red and 3 mirrors in blue), where each has six pixels. The base station and the mobile device on the user is fixed as illustrated in Fig. 4 (a).

2) APF Effect on Obstacles: First we want to present an example of the APF and its effect when it encounters an obstacle, and this is presented in Fig. 5. Each of the graph shows the APF from the base station to a mirror and onto the mobile device. Fig. 5 (a) show a very smooth APF gradient from the base station to the mobile device as the signals bounces off from mirror 1, which demonstrates that there is no obstacle blocking the path. Fig. 5 (b) show partial blockage in the APF, and this results in a rise in the APF for selected signal paths. Fig. 5 (c) shows a full blockage of the THz signals towards mirror 3 due to the obstacle that is right in the middle of the path.

3) THz SNR of the Personal Zone: Fig. 6 shows the maximum SNR of THz rays from each mirror with variation in the number of obstacles. The graph also shows the number of antenna strips that are used, where the case of no APF will lead to all antenna strips turned on resulting in high energy consumption. Fig. 6 (a) shows that using 3 mirrors, the result has certain outages when the number of obstacles is high. This means that the APF was not successful in determining an appropriate path between the base station and the mirror and to the mobile device. However, in Fig 6 (b) when using 6 mirrors, there are more available LoS possibilities, since the APF can find paths that go around the obstacles. Fig. 7 illustrates the number of signals that arrive at a user's Personal zone. The user is located in grid points (0, 0) on the x-y axis. Fig. 7 (a) is 50cm on each direction of the user, while Fig. 7 (b) is 100 cm. As shown in the figure, due to the position of the mobile (Fig. 4 (a)), there is higher number of signals that hits a region of the user from specific mirrors. This shows that quality and varying signal strengths will be experienced by the user with the help of the APF and the mirrors.

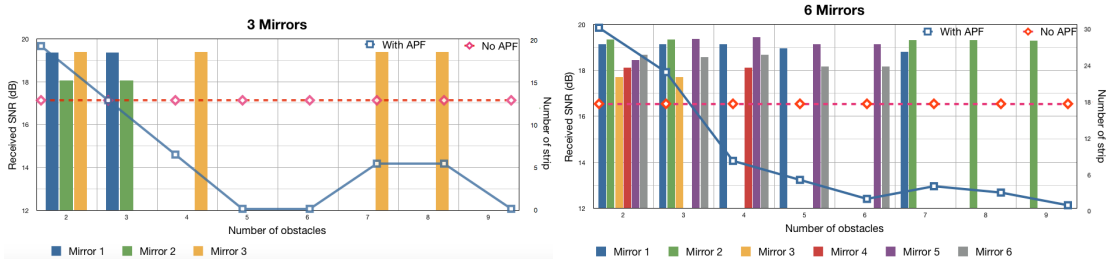

(a) (b)

Fig. 6: Maximum SNR from each mirror and number of antenna strips that are turned on for both (a) 3 mirrors, and (b) 6 mirrors. Dash line represents number of turned on antenna strips without information of APF and in the other hand, solid line with the information of APF.

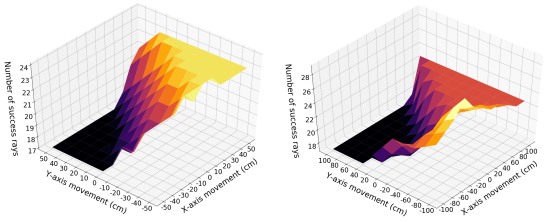

(a) (b)

Fig. 7: Number of signals inside personal zone with micro movements inside (a) 50 cm (b) 100 cm.

V. Conclusion

As the research community embarks on THz frequencies for future high speed wireless links, new solutions are continually being sought to meet the challenges of this specific spectrum band. A proposed approach that has gained attention recently is the use of reflectors, which could be simple mirrors or programmable materials, to redirect THz beams round obstacles. In this paper, we propose the use of an APF that can help guide the THz signals towards the mobile device of a user through the mirrors. The use of APF ensures that the antenna strip selected for emitting the beam will result in a clean path from the base station to the mobile user. The proposed approach also considers micro-movement of the user that can result in loss of connectivity, and this is through the multiple rays that will reflect off the mirrors to cover the user's Personal Zone. Simulation results have shown the effectiveness of the APF in assisting the THz signals to reach the mobile user, while also ensuring that only a small number of antenna strips are turned on to minimize energy consumption. Our proposed solution is a first step towards an autonomous THz environment that can provide high speed connections for users in face of varying blockages from obstacles.

Acknowledgement

This work was supported in part by the Finnish Academy Research Fellow Programme under Project 284531, and in part by the Science Foundation Ireland via the CONNECT Research Centre under Grant 13/RC/2077.

References

[1] C. Liaskos, S. Nie, A. Tsioliaridou, A. Pitsillides, S. Ioannidis, and I. Akyildiz, "A new wireless communication paradigm through software-controlled metasurfaces," *IEEE Communications Magazine*, vol. 56, pp. 162–169, Sept 2018.

[2] R. Daniels and R. Heath, "60 GHz wireless communications: Emerging requirements and design recommendations," *IEEE Vehicular Technology Magazine*, vol. 2, pp. 41–50, 9 2007.

[3] V. Petrov, M. Komarov, D. Moltchanov, J. M. Jornet, and Y. Koucheryavy, "Interference and sinr in millimeter wave and terahertz communication systems with blocking and directional antennas," *IEEE Transactions on Wireless Communications*, vol. 16, no. 3, pp. 1791–1808, 2017.

[4] S. Balasubramaniam and J. Kangasharju, "Challenges and requirements towards realizing internet of nano things," *Computer*, p. 1, 2012.

[5] M. T. Barros, R. Mullins, and S. Balasubramaniam, "Integrated terahertz communication with reflectors for 5g small-cell networks," *IEEE Transactions on Vehicular Technology*, vol. 66, no. 7, pp. 5647–5657, 2017.

[6] X. Tan, Z. Sun, D. Koutsonikolas, and J. M. Jornet, "Enabling indoor mobile millimeter-wave networks based on smart reflect-arrays," in *IEEE INFOCOM 2018-IEEE Conference on Computer Communications*, pp. 270–278, IEEE, 2018.

[7] L. Khamsawad, M. Pengnoo, P. Sasithong, P. Vanichchanunt, L. Wuttisittikulkij, M. T. Barros, and S. Balasubramaniam, "Simulation of signal coverage for terahertz communications," in *The 33rd International Technical Conference on Circuits/Systems, Computers and Communications (ITC-CSCC)*, 2018.

[8] C. Han, A. O. Bicen, and I. F. Akyildiz, "Multi-ray channel modeling and wideband characterization for wireless communications in the terahertz band," *IEEE Transactions on Wireless Communications*, vol. 14, no. 5, pp. 2402–2412, 2015.

[9] S. Priebe and T. Kurner, "Stochastic modeling of thz indoor radio channels," *IEEE Transactions on Wireless Communications*, vol. 12, no. 9, pp. 4445–4455, 2013.

[10] J. M. Jornet and I. F. Akyildiz, "Channel modeling and capacity analysis for electromagnetic wireless nanonetworks in the terahertz band," *IEEE Transactions on Wireless Communications*, vol. 10, no. 10, pp. 3211–3221, 2011.

[11] I. F. Akyildiz, J. M. Jornet, and C. Han, "Terahertz band: Next frontier for wireless communications," *Physical Communication*, vol. 12, pp. 16–32, 2014.

[12] C. Jansen, S. Priebe, C. Moller, M. Jacob, H. Dierke, M. Koch, and T. Kurner, "Diffuse scattering from rough surfaces in thz communication channels," *IEEE Transactions on Terahertz Science and Technology*, vol. 1, no. 2, pp. 462–472, 2011.

[13] P. Vadakkepat, K. C. Tan, and W. Ming-Liang, "Evolutionary artificial potential fields and their application in real time robot path planning," in *Evolutionary Computation, 2000. Proceedings of the 2000 Congress on*, vol. 1, pp. 256–263, IEEE, 2000.

[14] T. W. Dunbar and J. M. Esposito, "Artificial potential field controllers for robust communications in a network of swarm robots," in *System Theory, 2005. SSST'05. Proceedings of the Thirty-Seventh Southeastern Symposium on*, pp. 401–405, IEEE, 2005.

[15] "IEEE standard for high data rate wireless multi-media networks–amendment 2: 100 gb/s wireless switched point-to-point physical layer," *IEEE Std 802.15.3d-2017 (Amendment to IEEE Std 802.15.3-2016 as amended by IEEE Std 802.15.3e-2017)*, pp. 1–55, Oct 2017.